online data

Different phospholipase-C-coupled receptors differentially regulate capacitative and non-capacitative Ca^{2+} entry in A7r5 cells

Zahid MONEER, Irene PINO, Emily J. A. TAYLOR, Lisa M. BROAD[1], Yingjie LIU, Stephen C. TOVEY, Leila STAALI and Colin W. TAYLOR[2]

Department of Pharmacology, University of Cambridge, Tennis Court Road, Cambridge CB2 1PD, U.K.

Several receptors, including those for AVP (Arg^8-vasopressin) and 5-HT (5-hydroxytryptamine), share an ability to stimulate PLC (phospholipase C) and so production of IP_3 (inositol 1,4,5-trisphosphate) and DAG (diacylglycerol) in A7r5 vascular smooth muscle cells. Our previous analysis of the effects of AVP on Ca^{2+} entry [Moneer, Dyer and Taylor (2003) Biochem. J. **370**, 439–448] showed that arachidonic acid released from DAG stimulated NO synthase. NO then stimulated an NCCE (non-capacitative Ca^{2+} entry) pathway, and, via cGMP and protein kinase G, it inhibited CCE (capacitative Ca^{2+} entry). This reciprocal regulation ensured that, in the presence of AVP, all Ca^{2+} entry occurred via NCCE to be followed by a transient activation of CCE only when AVP was removed [Moneer and Taylor (2002) Biochem. J. **362**, 13–21]. We confirm that, in the presence of AVP, all Ca^{2+} entry occurs via NCCE, but 5-HT, despite activating PLC and evoking release of Ca^{2+} from intracellular stores, stimulates Ca^{2+} entry only via CCE. We conclude that two PLC-coupled receptors differentially regulate CCE and NCCE. We also address evidence that, in some A7r5 cells lines, AVP fails either to stimulate NCCE or inhibit CCE [Brueggemann, Markun, Barakat, Chen and Byron (2005) Biochem. J. **388**, 237–244]. Quantitative PCR analysis suggests that these cells predominantly express TRPC1 (transient receptor potential canonical 1), whereas cells in which AVP reciprocally regulates CCE and NCCE express a greater variety of TRPC subtypes (TRPC1 = 6 > 2 > 3).

Key words: capacitative Ca^{2+} entry, 5-hydroxytryptamine (5-HT), nitric oxide, vascular smooth muscle, vasopressin.

INTRODUCTION

In most cells, receptors that activate PLC (phospholipase C) stimulate both release of Ca^{2+} from intracellular stores and Ca^{2+} entry. The former is mediated by IP_3 (inositol 1,4,5-trisphosphate) receptors, and the latter is often thought to be mediated by CCE (capacitative Ca^{2+} entry), which is activated by depletion of intracellular Ca^{2+} stores [1]. CCE is not, however, the only Ca^{2+} entry pathway to be activated by PLC-linked receptors: additional NCCE (non-capacitative Ca^{2+} entry) pathways regulated by a variety of intracellular signals may be at least as important as CCE in some cell types [2,3].

A7r5 vascular smooth muscle cells express at least three distinct Ca^{2+} entry pathways. L-type Ca^{2+} channels are voltage-gated and are responsible for spontaneous Ca^{2+} spiking [4]; they were inhibited throughout the present study by either verapamil (10 μM) or nimodipine (100 nM). Depletion of intracellular stores causes activation of CCE [1]. In A7r5 cells, this pathway is permeable to Mn^{2+} and Ba^{2+}, but not to Sr^{2+}, and it is selectively blocked by a low concentration of Gd^{3+} (1 μM) or by 2-APB (2-aminoethoxydiphenyl borane; 100 μM) [5,6] (Figure 1a). The CCE pathways of many cells share this sensitivity to Gd^{3+} and 2-APB [7]. AVP (Arg^8-vasopressin), a potent vasoconstrictor that binds to the V_{1A} receptors of A7r5 cells [8] to stimulate formation of IP_3 and DAG (diacylglycerol), also activates an NCCE pathway [5,6,9]. Activation of NCCE does not require depletion of intracellular Ca^{2+} stores [5]. The pathway is permeable to Sr^{2+} and Ba^{2+}, but not to Mn^{2+}, and it is selectively blocked by LOE-908 {(*R*,*S*)-(3,4-dihydro-6,7-dimethoxyisochinolin-1-yl)-2-phenyl-*N*,*N*′-di[2-(2,3,4-trimethoxyphenyl)ethyl]acetamid mesylate} [6,10] and by a low concentration (100 nM) of SKF 96365 {1-[β-[3-(4-methoxyphenyl)propoxyl]-4-methoxyphenylethyl]-1*H*-imadazole hydrochloride} [11]. NCCE appears to be activated directly by NO produced when arachidonic acid released from DAG by DAG lipase activates NOS-III (type III nitric oxide synthase) [6,11] (Figure 1a). A similar mode of regulation of a similar NCCE pathway in insect pacemaker neurons was recently reported; here, the pathway is constitutively active, but is stimulated further by the PLC-linked adipokinetic hormone [12].

In addition to activating NCCE, AVP inhibits CCE via arachidonic acid, activation of NOS-III and then of PKG (cGMP-dependent protein kinase) [6,11] (Figure 1a). In other cells too, both arachidonic acid [13–17] and NO [18] have been reported to inhibit CCE, although the mechanisms include effects on both the CCE pathway itself [17] and its regulation [15,18]. Our initial study, however, reported no such inhibition of CCE by AVP [9], and recent studies likewise failed to detect inhibition of CCE by AVP [19,20]. We address these disparities in the present paper.

In our recent work, the Ca^{2+} entry evoked by AVP was mediated entirely by NCCE for as long as AVP was present, and this was followed by a burst of Ca^{2+} entry via CCE only when AVP was removed [6]. AVP, at both maximal and submaximal concentrations, thus evoked a sequential activation of first NCCE and then CCE. This led us to speculate that the Ca^{2+} signals arising

Abbreviations used: 2-APB, 2-aminoethoxydiphenyl borane; AVP, Arg^8-vasopressin; $[Ca^{2+}]_i$, intracellular free Ca^{2+} concentration; CCE, capacitative Ca^{2+} entry; C_T, cycle threshold; DAG, diacylglycerol; HBS, Hepes-buffered saline; HEK-293, human embryonic kidney; 5-HT, 5-hydroxytryptamine; IP_3, inositol 1,4,5-trisphosphate; LOE-908, (*R*,*S*)-(3,4-dihydro-6,7-dimethoxyisochinolin-1-yl)-2-phenyl-*N*,*N*′-di[2-(2,3,4-trimethoxyphenyl)ethyl]acetamid mesylate; NCCE, non-capacitative Ca^{2+} entry; NOS, nitric oxide synthase; PLC, phospholipase C; PKC, protein kinase C; PKG, cGMP-dependent protein kinase; RHC 80267, 1,6-bis(cyclohexyoximinocarbonylamino)hexane; SKF 96365, 1-[β-[3-(4-methoxyphenyl)propoxyl]-4-methoxyphenylethyl]-1*H*-imadazole hydrochloride; TBP, TATA-binding protein; TRPC, transient receptor potential canonical.

[1] Present address: Eli Lilly and Company Ltd, Lilly Research Centre, Erl Wood Manor, Sunningham Road, Windlesham, Surrey GU20 6PH, U.K.

[2] To whom correspondence should be addressed (email cwt1000@cam.ac.uk).

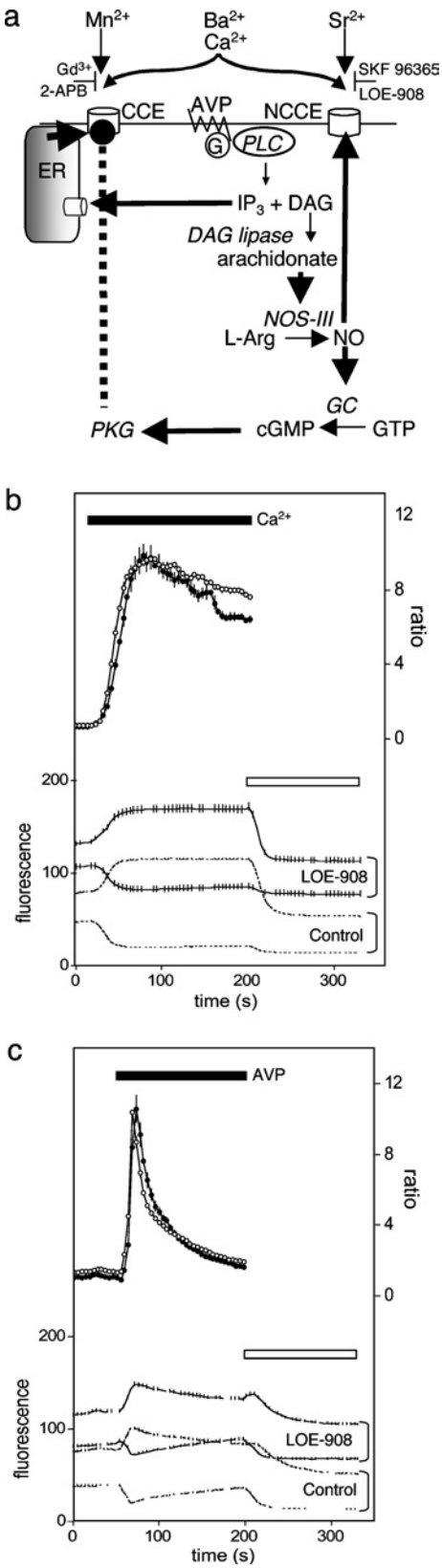

Figure 1 Reciprocal regulation of CCE and NCCE by AVP

(**a**) Signalling pathways linking AVP, via a G-protein and PLC, to emptying of intracellular stores by IP_3 and activation of NOS-III by arachidonate released from DAG. NO activates NCCE directly and via activation of soluble guanylate cyclase (GC), cGMP and consequent activation of PKG, it inhibits CCE. Hammerheads show selective inhibitors of CCE and NCCE.

(**b**, **c**) Fura 2 fluorescence recorded from A7r5 cells during CCE evoked by restoration of Ca^{2+} to thapsigargin-treated cells (**b**) or AVP-evoked release of Ca^{2+} from intracellular stores (**c**) in the presence (●) or absence (○) of LOE-908 (30 μM). In each panel, lower traces show fluorescence recorded after excitation at 340 or 380 nm (upper and lower traces of each pair respectively). Ionomycin (1 μM) and $MnCl_2$ (1 mM) were added at the time indicated by the open bar to quench fura 2 fluorescence. The upper traces show the fluorescence ratios (F_{340}/F_{380}) after correction for autofluorescence. Results are means ± S.E.M, $n \geqslant 15$.

from the two Ca^{2+} entry pathways may selectively regulate different physiological responses [6]. This pattern of regulation is consistent with both the mechanisms we propose for reciprocal regulation of the two pathways (Figure 1a) and with evidence that AVP activates only CCE when either DAG lipase [6] or NOS is inhibited (see Figure 3) [11]. It is not, however, entirely consistent with our earlier conclusion that both NCCE and CCE contribute to the Ca^{2+} entry evoked by a maximal concentration of AVP [5] and it is inconsistent with the conclusions of Brueggemann et al. [19] that there is no activation of CCE after AVP removal. In both studies [5,19], the Ca^{2+} entry evoked by a maximal concentration of AVP was also less sustained than in our recent work [6,11]. These issues: the relative roles of CCE and NCCE, and the duration of the response to AVP are also addressed in the present paper.

We establish that two receptors that share an ability to activate PLC nevertheless differentially regulate CCE and NCCE, and we consider likely reasons for the variability in receptor-regulated Ca^{2+} entry in different studies.

EXPERIMENTAL

Measurement of $[Ca^{2+}]_i$ (intracellular free Ca^{2+} concentration)

A7r5 cells were originally obtained from the American Type Culture Collection, but we have also obtained them from Dr H. De Smedt (University of Leuven, Leuven, Belgium), Dr K. L. Byron (Loyola University, Chicago, IL, U.S.A.), Dr A. P. Dawson (University of East Anglia, Norwich, U.K.) and Dr M. Lazdunski (University of Nice, Nice, France). Cells were cultured on glass coverslips, loaded with fura 2, mounted in a cuvette in the light path of a fluorescence spectrometer and excited at 340 and 380 nm, while collecting emitted light at 510 nm [6]. After correction for autofluorescence, calibration of fluorescence ratios ($R_{340/380}$) to $[Ca^{2+}]_i$ was performed using look-up tables created from Ca^{2+} standard solutions (Molecular Probes) [6,11]. Cells were continuously perfused (17 ml/min) at 20 °C with HBS (Hepes-buffered saline) containing: 135 mM NaCl, 5.9 mM KCl, 1.2 mM $MgCl_2$, 1.5 mM $CaCl_2$, 11.6 mM Hepes and 11.5 mM glucose, pH 7.3. The half-time for exchange of medium within the cuvette was 9.6 ± 0.3 s. All media included either verapamil (10 μM) or nimodipine (100 nM) to inhibit L-type Ca^{2+} channels. Mn^{2+} entry was measured in nominally Ca^{2+}-free HBS containing 200 μM $MnCl_2$, with fura 2 fluorescence excited at 360 nm [5]. In the most recent experiments (Figures 1b, 1c and 4), $[Ca^{2+}]_i$ was measured in fura-2-loaded A7r5 cells grown in 96-well plates using a fluorescence plate reader that allowed automated additions (Flexstation, Molecular Devices).

We, using fura 2 [6], and others, using fluo 3 [10], have reported that, in A7r5 cells, LOE-908 inhibits NCCE [6,10,19] without inhibiting CCE [21] (Figure 1b) or AVP-evoked Ca^{2+} release (Figure 1c). Although LOE-908 is fluorescent, it does not affect ratiometric measurements of fura 2 fluorescence in populations of A7r5 cells (Figures 1b and 1c). In later experiments, we used SKF 96365 (100 nM) selectively to inhibit NCCE, because it is more readily available than LOE-908 and it avoids any potential fluorescence problems: 100 nM SKF 96365 has no effect on fura 2

fluorescence (results not shown) and it does not affect CCE or AVP-evoked Ca^{2+} release [11], although, at a much higher concentration (10 μM), it does inhibit CCE [10].

Unless otherwise stated, traces are typical of at least three experiments, and results are shown as means ± S.E.M for at least three independent experiments.

Quantitative PCR

RNA was isolated directly from frozen A7r5 cells using Tri reagent (Sigma) according to the manufacturer's instructions, and cDNA was synthesized in a final volume of 20 μl from the RNA (1–5 μg) using the Superscript II first-strand synthesis kit (Invitrogen) primed with oligo$(dT)_{12-18}$.

For quantitative PCR, each reaction included LUX (light upon extension) primers [22] (Invitrogen) for a specific TRPC (transient receptor potential canonical) labelled with FAM (6-carboxyfluorescein) and, to allow calibration, primers for a housekeeping gene labelled with JOE (6-carboxy-5′,5′-dichloro-2′,7′-dimethoxyfluorescein), either β-actin or TBP (TATA-binding protein). Each reaction mixture (25 μl) contained 1 μl of A7r5 cDNA, 0.5 μM TRPC-specific primer pair (see Supplementary Table S1 at http://www.BiochemJ.org/bj/389/bj3890821add.htm), primer pairs (Invitrogen) for either TBP (0.5 μM) or β-actin (0.06 μM), Jumpstart real-time PCR mix (Sigma) and 3 mM $MgCl_2$. For PCRs (Corbett RG 3000), an initial denaturation at 93 °C for 2 min was followed by 40 cycles of amplification (93 °C for 10 s, 60 °C for 15 s and 72 °C for 20 s). Reaction mixtures were then incubated at 72 °C for 2 min and then ramped to 99 °C to obtain a melting-curve analysis. The latter was used to confirm the authenticity of all PCR products. Fluorescence was monitored during every PCR cycle at the extension step, and then at 1 °C intervals during the temperature ramp of the melting curve. Conditions were optimized to ensure similar amplification efficiencies for all products.

For every PCR, the C_T (cycle threshold) for each TRPC product was normalized to C_T for either of the housekeeping (HK) products (β-actin or TBP) ($\Delta C_T = C_T^{TRPC} - C_T^{HK}$) [23]. Assuming 100 % efficiency for each PCR cycle, ΔC_T can be converted into a relative REL (RNA expression level) from $REL = 2^{-\Delta CT}$ [23].

Membrane fractionation and immunoblotting

A confluent flask (150 cm^2) of A7r5 cells was washed in PBS, which were scraped into 500 mM Na_2CO_3 at pH 11 (1 ml), homogenized, sonicated and then mixed with 1 ml of 90 % sucrose in 25 mM Mes and 150 mM NaCl, pH 6.5. Lipid rafts were then separated from other membrane compartments using a discontinuous sucrose gradient [24,25]. The sample (2 ml) was over-layered with 1.5 ml of 35 % sucrose and 1 ml of 5 % sucrose (each in 25 mM Mes, 150 mM NaCl and 250 mM Na_2CO_3, pH 6.5). After centrifugation (Beckman SW55 rotor at 24 000 rev./min for 16 h at 4 °C), samples (250 μl) were collected for immunoblotting and analysis of sucrose concentration by refractometry.

For immunoblotting, samples (13 μl) were separated by SDS/PAGE on 4–12 % Bis-Tris gradient gels (Invitrogen), transferred to Immobilon membranes (Millipore), blocked and incubated with primary and secondary antisera using standard methods. The primary antibodies were: monoclonal against caveolin-1 (1:1000), caveolin-3 (1:5000), NOS-III (1:1000) and 5-HT_{2A} (5-hydroxytryptamine) receptor (1:100) (all BD Biosciences), and goat polyclonal antisera against V_{1A} vasopressin receptor (1:100; Santa Cruz Biotechnology) and β-adaptin (1:1000; Santa Cruz Biotechnology). HRP (horseradish peroxidase)-conjugated secondary antibodies were used: goat anti-mouse (1:2000; Sigma) and donkey anti-goat (1:1000; AbCam). Immunoreactivity was detected using SuperSignal West Pico Chemiluminescent substrate (Pierce) and bands were then quantified using GeneTools (Gene Gnome, Syngene, Cambridge, U.K.).

Materials

Ketanserin was from Sigma. LOE-908 was a gift from Boehringer-Ingelheim. Sources of all other materials were provided in previous publications [6,11].

RESULTS

Inhibition of CCE by AVP

In A7r5 cells, the increase in $[Ca^{2+}]_i$ evoked by CCE is decreased by AVP [5,6,9,11,26] (Figure 2c). Although we had initially assumed that this decrease in $[Ca^{2+}]_i$ was due to a PLC-independent activation of Ca^{2+} extrusion [26], retrospective analysis of data showing that arachidonic acid does not stimulate Mn^{2+} entry via the NCCE pathway (Figure 1a) [5] shows also that AVP (Figure 2b) and arachidonic acid (Figure 2e) inhibit CCE. In each of two experiments, AVP (100 nM) inhibited the rate of Mn^{2+} entry into cells with empty stores by 43 % (Figure 2b), while arachidonic acid (50 μM) inhibited it by 57 ± 7 % ($n = 3$). These results (from 1998) are consistent with our later conclusion (in 2002) that AVP, via arachidonic acid, inhibits CCE [6] (Figure 1a). However, in parallel experiments, empty stores stimulated Ba^{2+} entry that was increased further by AVP (Figure 2a). The result with Ba^{2+} is similar to that reported in [9], but different from that in our later report where AVP inhibited Ba^{2+} entry [6].

A likely explanation for the different results with Ba^{2+} and Mn^{2+} comes from the observation that, whereas Mn^{2+} permeates only the CCE pathway and so reports only its activity, Ba^{2+} permeates both CCE and NCCE pathways (Figure 1a) [9]. The effect of AVP on Ba^{2+} entry is thus a balance between inhibition of its entry via CCE and stimulation of its entry via NCCE. Net Ba^{2+} entry therefore depends on the relative Ba^{2+} permeabilities of the two pathways, their expression levels and their activities. Mn^{2+} quench of fura 2 fluorescence thus provides a more selective means of assessing whether AVP inhibits CCE in A7r5 cells. Nevertheless, it is clear that, in some A7r5 cell lines, AVP fails to inhibit capacitative Mn^{2+} entry [9,19]. We return to this issue below.

Reciprocal regulation of CCE and NCCE by AVP

Figure 3 confirms the key features of the Ca^{2+} entry evoked by AVP. AVP stimulated an initial release of Ca^{2+} from intracellular stores, which was complete within approx. 100 s, and this was followed by a sustained phase of Ca^{2+} entry (Figure 3a). The latter was blocked completely by SKF 96365 (100 nM), but unaffected by Gd^{3+} (1 μM) (Figure 3b). This is consistent with earlier work showing that, in the presence of AVP, Ca^{2+} entry occurs entirely via NCCE [6]. Inhibition of DAG lipase {with RHC 80267 [1,6-bis(cyclohexyoximinocarbonylamino)hexane]} [27] increased the amplitude of the Ca^{2+} entry evoked by AVP and changed its pharmacological properties, such that it became insensitive to SKF 96365 and was blocked completely by Gd^{3+} (Figure 3b). Inhibition of NOS, which lies downstream of arachidonic acid (Figure 1a), likewise both increased the amplitude of the Ca^{2+} entry evoked by AVP and switched it from NCCE to CCE (Figure 3b). These and previous results [5,6,11] support the scheme shown in Figure 1(a), where all Ca^{2+} entry in the presence of AVP occurs via NCCE, because the arachidonic acid released from DAG activates NOS-III. The NO produced then activates NCCE directly, and via activation of soluble guanylate cyclase and PKG, it inhibits CCE [11].

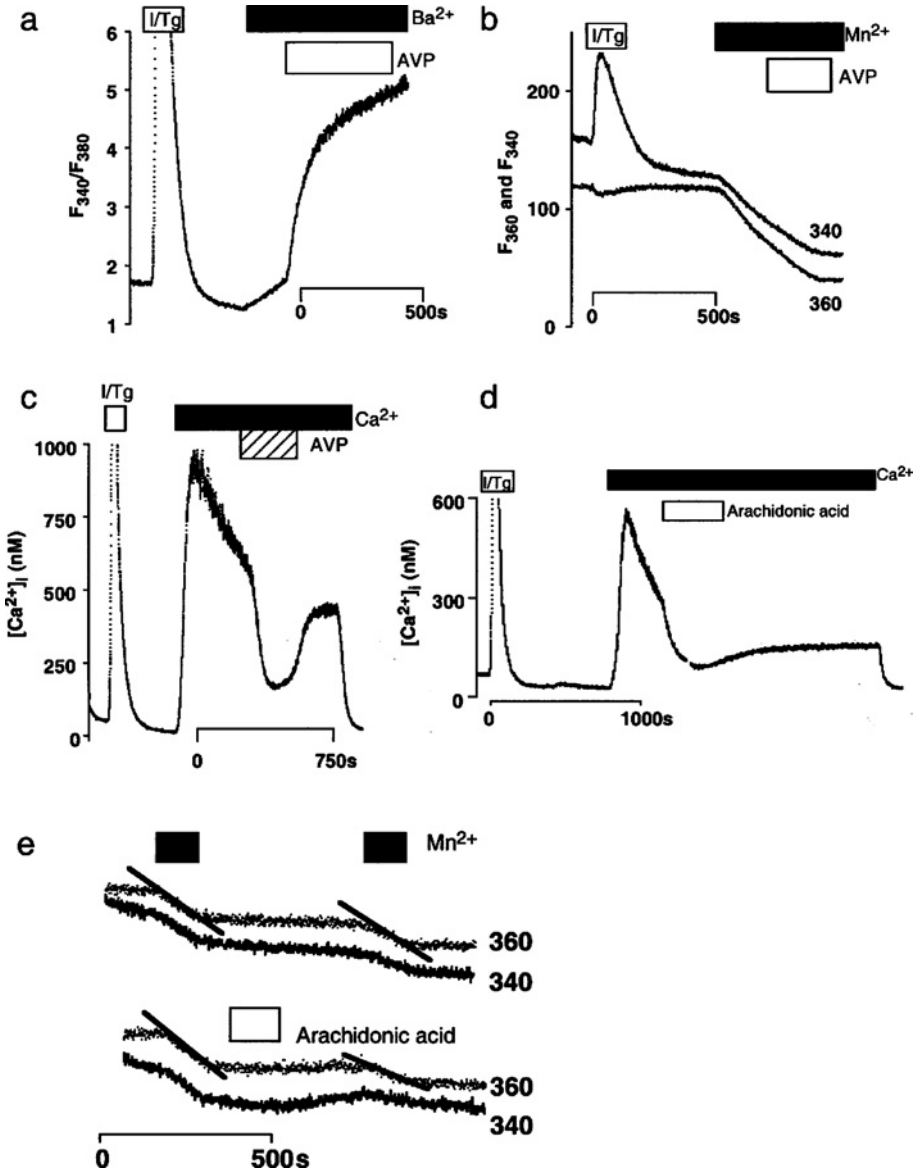

Figure 2 Effects of AVP on capacitative Mn^{2+} and Ba^{2+} entry

(**a**, **b**) In parallel experiments, normal A7r5 cells were treated with ionomycin and thapsigargin (I/Tg; 1 μM of each) to activate CCE causing an increase in Ba^{2+} (**a**) and Mn^{2+} (**b**) entry. Subsequent addition of AVP (100 nM) increased Ba^{2+} entry further, but inhibited Mn^{2+} entry, whether recorded using fluorescence excited at 340 or 360 nm. (**c**) AVP (100 nM) reversibly decreased the increase in $[Ca^{2+}]_i$ evoked by CCE in normal A7r5 cells. (**d**) Even in cells lacking DAG lipase activity, arachidonic acid (20 μM) reversed the increase in $[Ca^{2+}]_i$ evoked by CCE. (**e**) In normal cells, arachidonic acid (20 μM) inhibited Mn^{2+} entry via CCE. The persistent effect of arachidonic acid in these experiments (**d**, **e**), which occurred also in parallel measures of Sr^{2+} entry (results not shown), probably results from slow washout of arachidonic acid from the perfusion apparatus. Representative traces are shown, each typical of $\geqslant 3$ (**a**–**c**) or 2 (**d**, **e**) similar experiments.

Regulation of CCE and NCCE by 5-HT and AVP

A maximal concentration of 5-HT stimulated both release of Ca^{2+} from intracellular stores and Ca^{2+} entry (Figures 4a and 5c–5e). Both responses were mimicked by α-methyl-5-HT (a selective agonist of 5-HT_{2A-C} receptors) and blocked by ketanserin (100 nM; a selective antagonist of 5-HT_{2A} receptors) (results not shown). The exclusive involvement of 5-HT_{2A} receptors was established using Schild analysis, which showed that the receptor through which 5-HT evoked Ca^{2+} signals had an affinity (K_d) for ketanserin of 1.19 nM (Figure 4b). This confirms the requirement for 5-HT_{2A} receptors [28], activation of which is known to stimulate PLC.

In parallel experiments, the amplitude of the Ca^{2+} entry evoked by 5-HT was much larger than that evoked by AVP and it also had the opposite sensitivity to Gd^{3+} and SKF 96365 (Figure 5c). Gd^{3+} blocked the Ca^{2+} entry evoked by 5-HT without affecting that evoked by AVP, whereas SKF 96365 had the opposite effects, blocking the Ca^{2+} entry evoked by AVP without affecting that evoked by 5-HT. Similar results were obtained with a submaximal concentration of 5-HT (Figure 5d). These results establish that, whereas AVP stimulates Ca^{2+} entry only via NCCE, 5-HT stimulates Ca^{2+} entry only via CCE (Figures 5a–5d). We commented previously that 5-HT stimulated Sr^{2+} entry (i.e. NCCE; see Figure 1a) [5,6], but the amplitudes of these Sr^{2+} signals were $< 15\,\%$ of those evoked by AVP. This does not

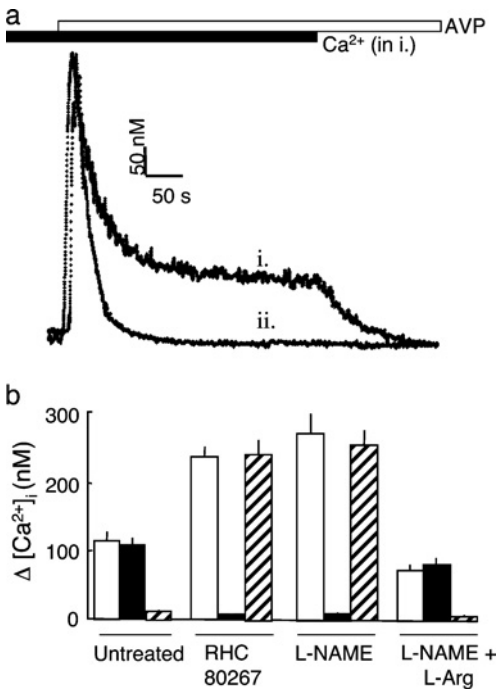

Figure 3 Reciprocal regulation of CCE and NCCE via arachidonic acid and NO

(**a**) Increases in $[Ca^{2+}]_i$ evoked by AVP (100 nM, open bar) in the presence (i, solid bar) and absence (ii) of extracellular Ca^{2+}. (**b**) Increases in $[Ca^{2+}]_i$ recorded 240 s after the addition of AVP (100 nM) are shown for control cells or after pre-treatment with RHC 80267 (50 μM to inhibit DAG lipase), L-NAME (N^G-nitro-L-arginine methyl ester; 700 μM to inhibit NOS) or L-NAME with L-arginine (2.1 mM). Open bars denote responses in the absence of channel blockers, solid bars show responses in the presence of 1 μM Gd^{3+} to inhibit CCE, and hatched bars show responses in the presence of 100 nM SKF 96365 to inhibit NCCE. Results are means $\pm$ S.E.M for three independent experiments.

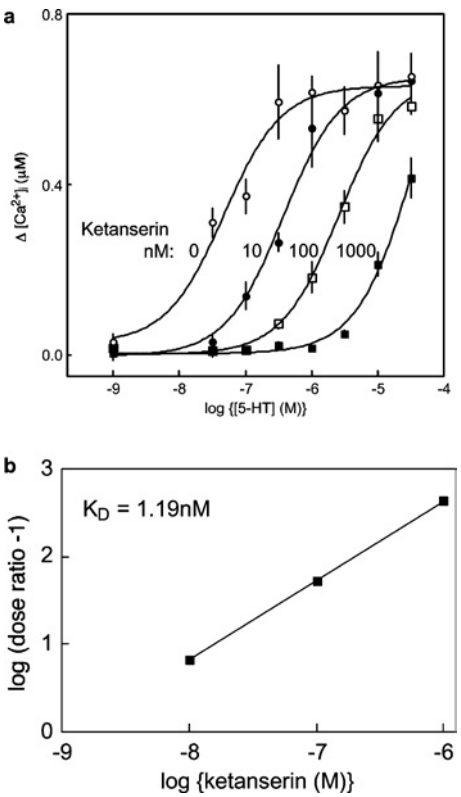

Figure 4 Competitive inhibition of 5-HT-evoked Ca^{2+} signals by ketanserin

(**a**) Cells in HBS were pre-incubated (30 s) with the indicated concentrations of ketanserin before addition of 5-HT. The curves show the peak increases in $[Ca^{2+}]_i$ evoked by each concentration of 5-HT in the presence of 0, 10, 100 or 1000 nM ketanserin. (**b**) Schild analysis of the results (dose ratio = EC_{50} in the presence of ketanserin/EC_{50} in its absence) establishes that the affinity (K_d) of the receptor through which 5-HT exerts its effects on $[Ca^{2+}]_i$ is 1.19 nM. In these experiments, $[Ca^{2+}]_i$ was measured using a Flexstation fluorescence plate reader. Results are means $\pm$ S.E.M for three independent experiments.

therefore conflict with the present results, where so small a Ca^{2+} signal mediated by NCCE (<20 nM; Figures 3a and 4a) would not be easily resolved (Figure 5).

The Ca^{2+} responses to both AVP and 5-HT were abolished by U73122, an inhibitor of PLC [29], and each was similarly sensitive to it: the IC_{50} (half-maximal inhibitory concentration) for U73122 was 607 ± 367 nM for AVP (1 μM) and 428 ± 196 for 5-HT (50 μM) (results not shown).

The concentration-dependence of the effects of the two agonists on Ca^{2+} signals (Figure 5e) reveals that, even when their concentrations were adjusted so that each evoked comparable release of Ca^{2+} from intracellular stores (presumably reflecting comparable formation of IP_3), they still had very different effects on Ca^{2+} entry. AVP evoked a small NCCE, while 5-HT evoked a large CCE (Figure 5f). We conclude that two agonists, each sharing an ability to evoke an increase in $[Ca^{2+}]_i$ via stimulation of PLC, nevertheless exert very different effects on Ca^{2+} entry: in the presence of AVP, only NCCE is active, while only CCE is active in the presence of 5-HT.

Distribution of 5-HT_{2A} and V_{1A} receptors relative to lipid rafts

Figure 6 compares the distribution of caveolins-1 and 3 with 5-HT_{2A} and V_{1A} receptors in membrane fractions of A7r5 cells separated on a discontinuous sucrose gradient. Caveolins 1 and 3, along with NOS-III, were concentrated in less dense sucrose fractions, as expected for both lipid rafts and caveolae. However, both V_{1A} and 5-HT_{2A} receptors, although not excluded from the caveolin-rich fractions, were present in larger amounts in the non-caveolar fractions. The distribution of both receptors was similar to that of β-adaptin (Figure 6b), which is known to be excluded from caveolae [30]. There was no obvious difference in the distributions of the two receptors between membrane fractions of unstimulated A7r5 cells (Figure 6c).

Expression of TRPC proteins in A7r5 cells

Because the Ca^{2+} entry pathways of A7r5 cells appear to change unpredictably during culture, we used quantitative PCR to examine expression of TRPC proteins, as candidates for Ca^{2+}-entry channels [31,32] (see Supplementary Table S1 at http://www.BiochemJ.org/bj/389/bj3890821add.htm). We used RNA extracted directly from cells frozen in liquid nitrogen, where the behaviour of the Ca^{2+} entry pathways had been characterized immediately before the cells were frozen. Simultaneous measurements of RNA for two housekeeping proteins, one expressed at low level (TBP) and another at a higher level (β-actin), were used to calibrate the analyses of TRPC expression. Comparison of RNA levels for the housekeeping proteins within and between cell lines established that they provided reliable and consistent benchmarks for calibration of TRPC expression (see Supplementary Table S2 at http://www.BiochemJ.org/bj/389/bj3890821add.htm).

Expression levels for each TRPC mRNA relative to mRNA for β-actin (ΔC_T) in each of six cell lines, four with and two without AVP-regulated NCCE, are summarized in Supplementary Tables S3 and S4 (see http://www.BiochemJ.org/bj/389/

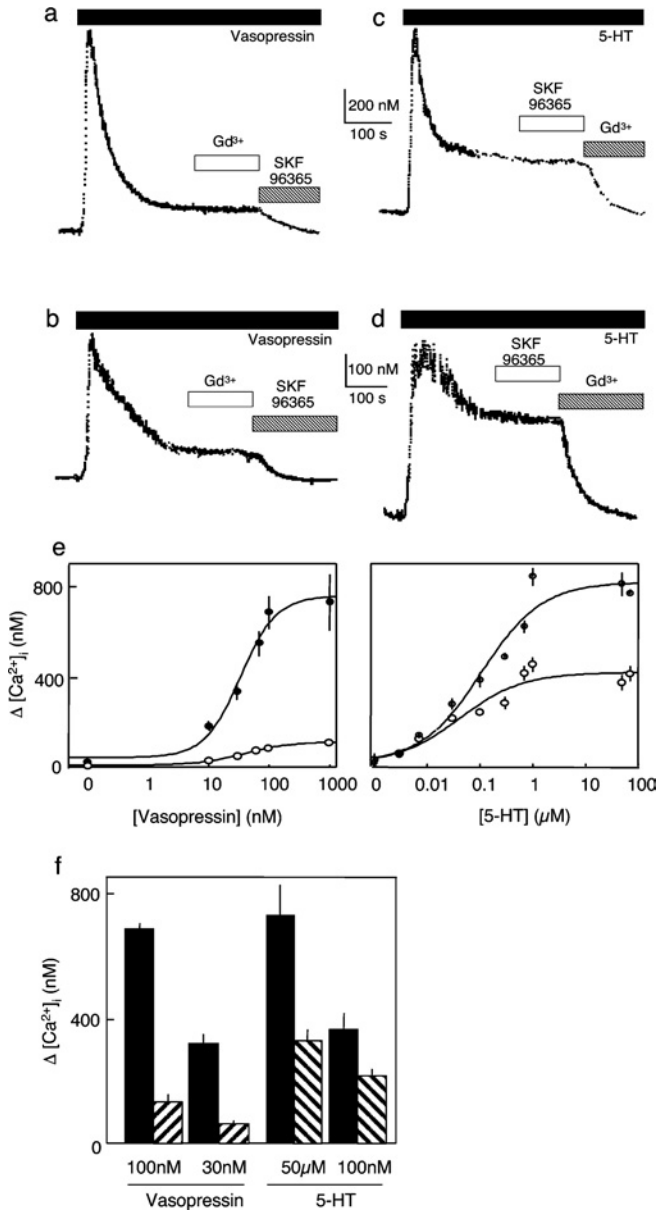

Figure 5 AVP and 5-HT stimulate different Ca^{2+} entry pathways

(**a**–**d**) Cells were stimulated with maximal (**a**, **c**) or submaximal (**b**, **d**) concentrations of AVP (30 and 100 nM) or 5-HT (100 nM and 50 μM) before the addition of SKF 96365 (100 nM) or Gd^{3+} (1 μM) as indicated. (**e**) Concentration-dependent effects of AVP and 5-HT on Ca^{2+} release from intracellular stores (●) and Ca^{2+} entry (○). (**f**) Comparison of the effects of concentrations of 5-HT and AVP that evoke comparable release of Ca^{2+} from intracellular stores (filled bars) on Ca^{2+} entry (hatched bars). Note that SKF 96365 (100 nM) abolished the Ca^{2+} entry evoked by AVP, without affecting that evoked by 5-HT, whereas Gd^{3+} (1 μM) had the opposite effect.

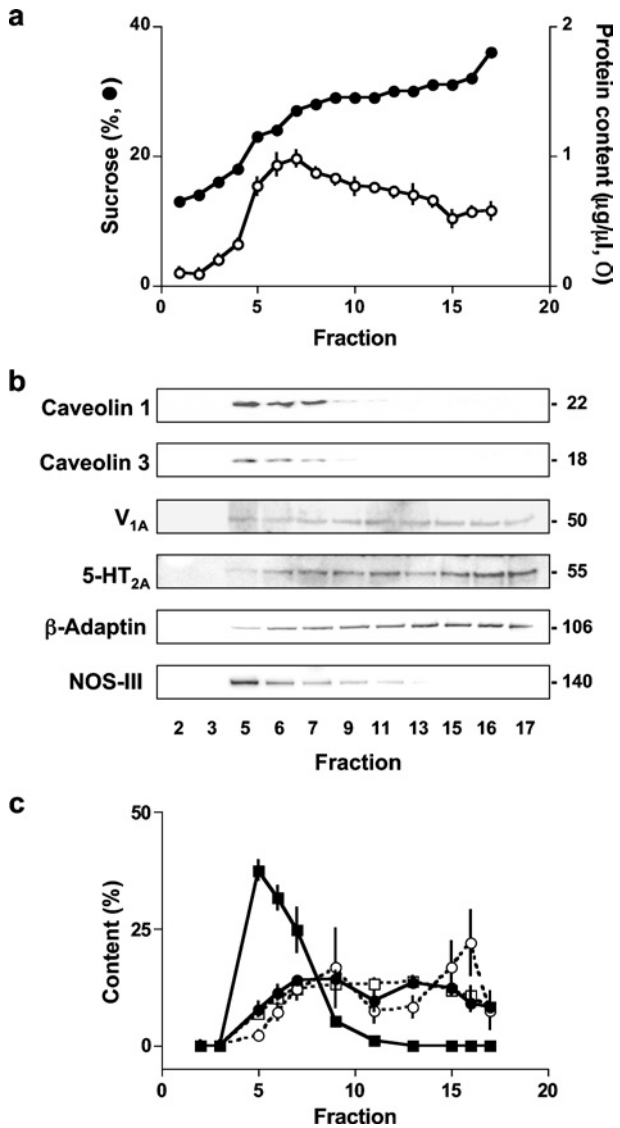

Figure 6 Distribution of V_{1A} and $5\text{-}HT_{2A}$ receptors and caveolins in membrane fractions

Membranes of A7r5 cells were fractionated on sucrose gradients (see the Experimental section) and fractions of 250 μl were collected. (**a**) Sucrose concentration (●) and protein content (○) of each fraction. (**b**) Representative Western blots for samples of 13 μl from the indicated fractions. The M_r of each band is shown calculated from the migration of standard M_r markers (MagicMarker-XP, Invitrogen). The $5\text{-}HT_{2A}$ antiserum identified two similarly intense bands with M_r ~55 and ~65; the lower band was used for quantification. (**c**) Results from three independent experiments (means ± S.E.M) are summarized with the intensity of caveolin 1 (■), V_{1A} receptor (●), $5\text{-}HT_{2A}$ receptor (○) and β-adaptin (□) bands each expressed as a percentage of the sum of the intensities of the bands across the entire gel.

bj3890821add.htm). In keeping with previous analyses of TRPC expression in A7r5 cells [33] and vascular smooth muscle [34,35], mRNAs for TRPC1 and TRPC6 were expressed at the highest levels in A7r5 cells and each was expressed at a similar level, there was lesser expression of TRPC2, 3 and 4, and extremely low (TRPC5) or undetectable (TRPC7) expression of the remaining subtypes (Table 1). In our limited comparison of cells with and without AVP-regulated NCCE, TRPC1 expression was unchanged, but expression of the major TRPC subtypes (TRPC2, 3 and 6) was massively reduced in cells without NCCE (Table 1).

DISCUSSION

Sustained and transient responses to AVP

Negative feedback by PKC (protein kinase C) desensitizes responses to AVP [5,36], and there may also be an additional more-specific inhibition of NCCE by PKC, because NCCE is more completely inhibited than AVP-evoked Ca^{2+} release [26]. This is consistent with evidence that another non-selective cation channel formed by TRPC3 is phosphorylated at a conserved site and thereby inhibited by PKC [37]. Feedback regulation by PKC may thus affect the amplitude and duration of the Ca^{2+} signals

Table 1 Expression of TRPC RNA in A7r5 cells with and without AVP-regulated NCCE

From the data presented in Supplementary Table S3 (see http://www.BiochemJ.org/bj/389/bj3890821add.htm), relative expression levels of mRNA for each TRPC were calculated in cells with (cell lines 94, 114, 244 and 250) and without (cell lines 264 and 381) reciprocal regulation of CCE and NCCE by AVP. All transcripts are expressed as percentages of TRPC1 expression in cells with NCCE. Values in parentheses show expression of each TRPC subtype as a percentage of total TRPC expression in that category of cell line. Results are means ± S.E.M.

	Expression relative to TRPC1 in cells with NCCE (%)						
	TRPC1	TRPC2	TRPC3*	TRPC4	TRPC5	TRPC6	TRPC7†
With NCCE	100	50 ± 26	23 ± 10	11 ± 3.4	2.0 ± 1.0	99 ± 24	< 0.008
	(35 ± 14)	(17 ± 6)	(8 ± 2)	(4 ± 1)	(0.7 ± 0.4)	(35 ± 5)	(≪1)
Without NCCE	90 ± 71	< 5	< 0.006	1.8 ± 0.9	0.27 ± 0.22	2.3 ± 0.1	< 0.008
	(86 ± 7)	(3 ± 3)	(≪1)	(6 ± 5)	(1 ± 1)	(6 ± 4)	(≪1)

* The primers for TRPC3 apparently interfered with amplification of the β-actin PCR product. Therefore, in these reactions only, TRPC3 and β-actin were quantified in parallel assays of the same RNA extracts. In the cell lines (264 and 381) where TRPC3 was not detected after 43 cycles, C_T values for β-actin were 25 and 27 respectively.

† In all cell lines, TRPC7 product was not detected after 40 cycles, and, in cell line 381, TRPC2 was undetected after 40 cycles. C_T for β-actin in these reactions was 23 ± 2 (for TRPC7) and 24.9 ± 0.3 (for TRPC2).

evoked by AVP. We suggest that differences in the extent of this feedback may have contributed to the different responses to AVP in different studies, where sustained Ca^{2+} entry signals evoked by maximal concentrations of AVP were undetectable [9], small [5,38] or substantial [6].

Comparison of the results shown in Figures 6(A) and 7 of [19], each showing responses to a maximal concentration of AVP, is instructive. The sustained increase in $[Ca^{2+}]_i$ evoked by AVP in Ca^{2+}-containing medium is small (much smaller than the CCE signal evoked by thapsigargin), but the initial increase in $[Ca^{2+}]_i$ evoked by AVP is much larger in Ca^{2+}-containing (~790 nM) than in Ca^{2+}-free (~290 nM) medium. This suggests that the initial response to AVP includes a significant contribution (~60 %, $\Delta[Ca^{2+}]_i$ ~500 nM) from Ca^{2+} entry, but that within minutes this rapidly decays [19] (perhaps reflecting the PKC-mediated desensitization described above). In the face of such desensitization, the initial response to AVP provides the clearest insight into the relative roles of CCE and NCCE in mediating AVP-evoked Ca^{2+} entry. AVP causes $[Ca^{2+}]_i$ to increase by ~790 nM, by ~600 nM when CCE is inhibited with 1 μM Gd^{3+}, and by only ~200 nM when NCCE is inhibited with LOE-908 [19]. The latter is similar to the response evoked in Ca^{2+}-free medium, suggesting a major role for NCCE. The insignificant effect of Gd^{3+} suggests a minimal role for CCE. These results agree with our conclusion that, when AVP is present, NCCE provides the major route for AVP-evoked Ca^{2+} entry [6]. The absence of significant CCE, despite initial emptying of intracellular stores, suggests further that AVP has inhibited CCE, although this is difficult to reconcile with results from the same authors showing that AVP fails to inhibit capacitative Mn^{2+} entry [19]. If, as we suggest, desensitization underlies the small sustained responses to AVP, late removal of AVP would not be expected to have any effect. It is unsurprising therefore that removal of AVP after 5 min fails [19] to trigger the transient CCE observed in our earlier work [6].

We conclude that recent work [19] supports our conclusion that NCCE provides the major route for Ca^{2+} entry in the presence of AVP [6], and that different (albeit unexplained) rates of feedback inhibition by PKC may influence the duration of the sustained Ca^{2+} signals evoked by AVP in different studies.

Receptor-specific regulation of CCE and NCCE

Two receptors (V_{1A} and 5-HT_{2A}), each using PLC to evoke a Ca^{2+} signal, have very different effects on Ca^{2+} entry. AVP stimulates Ca^{2+} entry via NCCE, while 5-HT stimulates Ca^{2+} entry via CCE (Figure 5). A rather similar situation exists in sympathetic neurons where muscarinic and bradykinin receptors are each coupled to PLC and each can activate TRPC6 via DAG, but only bradykinin (via IP_3-mediated depletion of intracellular stores) activates TRPC1 [39]. Here, it seems that IP_3 receptors in close proximity to bradykinin receptors allow bradykinin, but not muscarinic agonists, effectively to release intracellular Ca^{2+} stores.

In A7r5 cells, the reciprocal regulation of CCE and NCCE by AVP depends upon activation of NOS-III (Figure 1a), which is often concentrated in caveolae (Figure 6b) [40]. In contrast, responses to 5-HT (Figure 5) are similar to those evoked by AVP after inhibition of NOS-III (Figure 3). We therefore considered whether the spatial organization of V_{1A} and 5-HT_{2A} receptors might underlie the selective ability of V_{1A} receptors to communicate via arachidonic acid and NO with CCE and NCCE. Our results show that neither V_{1A} nor 5-HT_{2A} receptors are concentrated in lipid rafts, and neither are there obvious differences in the distribution of the two receptors between membrane fractions. A simple co-localization of V_{1A} receptors with NOS-III in caveolae is unlikely therefore to account for the selective ability of AVP to reciprocally regulate CCE and NCCE via NO (Figure 6b). There may, of course, be more subtle spatial determinants of the interactions between V_{1A} receptors and NOS-III, or it may be that, while both V_{1A} and 5-HT_{2A} receptors share an ability to stimulate PLC, only the former activates DAG lipase to promote release of arachidonic acid from DAG (Figure 1a).

Whatever the mechanism, it is clear that different receptors, despite sharing similar initial links with the Ca^{2+} signalling pathways, succeed in stimulating very different patterns of Ca^{2+} entry, which may then have very different functional consequences [41].

Different patterns of Ca^{2+} entry in different A7r5 cell lines

Different receptors differentially regulate CCE and NCCE (Figure 5), but why should different A7r5 cell lines differ in whether AVP reciprocally regulates the two pathways? We [6] and now others [19] have reported that AVP does not inhibit CCE in all A7r5 cell lines, and neither do all cell lines show activation of NCCE by AVP [5,6,20]. These features were originally found in only a minority of our A7r5 cell lines, but they have become more common in cells from different sources. Loss of DAG lipase probably accounts for the loss of reciprocal regulation of CCE and NCCE by AVP in some cells (Figure 1a) [5,6]. However, we have not succeeded in measuring directly DAG lipase activity in A7r5 cells labelled with [^{3}H]arachidonic acid (Y. Liu and C. W. Taylor, unpublished work), and, because the enzyme has not been isolated, its expression cannot be examined using PCR

or antibody methods. We have not therefore been able to establish directly whether levels of DAG lipase are altered in cells where AVP fails reciprocally to regulate CCE and NCCE. Changes in the extent to which PKC rapidly feeds back to inhibit AVP-evoked Ca^{2+} signals may also determine whether AVP evokes a substantial Ca^{2+}-entry signal.

Recently, we identified variants of A7r5 cells in which AVP failed to either inhibit CCE or stimulate NCCE; and arachidonic acid, an NO-donor (NOC-18), or 8-Br-cGMP failed to restore the regulation (results not shown). Loss of DAG lipase cannot explain this behaviour (Figure 1a), and, because signals (NO and 8-Br-cGMP; Figure 1a) that are thought to be very close to channel regulation were ineffective, we considered whether changes in the channels themselves might underlie the change in behaviour of both CCE and NCCE.

From our PCR analysis of RNA isolated from cells with and without AVP-regulated NCCE, the most striking difference between the cells is the massive decrease in expression of TRPC2, 3 and 6 in cells without reciprocal regulation of CCE and NCCE by AVP (Table 1). Almost 90 % of TRPC expressed in these cells is TRPC1, whereas cells in which AVP stimulates NCCE and inhibits CCE express a more balanced mixture of the major TRPC subtypes: ~35 % TRPC1, 35 % TRPC6, 16 % TRPC2 and 7 % TRPC3 (Table 1), suggesting that these cells are perhaps more likely to express hetero-oligomeric TRPC channels [42].

It is noteworthy that, in other cells, a change in expression of a single TRPC protein has been reported to change the properties of both CCE and NCCE pathways, suggesting that the different channels may share some TRPC subunits. In HEK-293 (human embryonic kidney) cells, for example, overexpression of TRPC3 does not increase the amplitude of CCE, yet it both modifies its behaviour by suppressing its sensitivity to Gd^{3+}, NO and mitochondrial uncouplers and increases receptor-regulated Ca^{2+} entry via NCCE [43,44]. In DT40 cells too, TRPC3 can both modulate the behaviour of endogenous CCE and contribute to NCCE [32]. We tentatively suggest therefore that hetero-oligomers of TRPC proteins may contribute to formation of both CCE and NCCE in A7r5 cells, and that the composition of the channel determines its susceptibility to inhibition by PKG (for CCE) and activation by NO (for NCCE).

We do not yet understand the mechanisms that lead to changes in the Ca^{2+} entry pathways of A7r5 cells, which may include changes in the behaviour and/or expression of PKC, DAG lipase and TRPC proteins, but it is clear that they are not restricted to A7r5 cells. During idiopathic pulmonary artery hypertension, for example, expression of TRPC3 and 6 is increased in vascular smooth muscle [35]. HEK-293 cells are another cell type where interactions between two Ca^{2+} entry pathways, NCCE (I_{ARC}, activated directly by arachidonic acid) and CCE, have been suggested to be important in determining the physiological route for Ca^{2+} entry. But different studies differ in whether arachidonic acid does [16] or does not [45] inhibit CCE, and in whether NCCE [3] or CCE [46] is responsible for sustaining Ca^{2+} oscillations. These disparities also remain unexplained, but serve further to highlight the need to understand both where and how differences arise in the signalling sequences linking receptors to distinct Ca^{2+} entry pathways [47].

In summary, we have shown that, whereas AVP can reciprocally regulate CCE and NCCE via NO; in the same cells, 5-HT causes only activation of CCE. The difference, which may allow two PLC-coupled receptors selectively to direct Ca^{2+} to different intracellular effectors, appears not to result from differential concentration of the two receptors within lipid rafts. We and others have reported that AVP fails to reciprocally regulate CCE and NCCE in some A7r5 cell lines and that loss of DAG lipase cannot adequately account for the behaviour of all such variant lines. We suggest that changes in expression of TRPC subtypes may also contribute to changes in the regulation of CCE and NCCE, with reciprocal regulation of the two pathways occurring in cells most likely to express hetero-oligomeric TRPC channels.

This work was supported by grants from the BBSRC (Biotechnology and Biological Sciences Research Council) and Wellcome Trust (072084). We thank Boehringer-Ingelheim for the gift of LOE-908, and Dr Sarah Lummis (Department of Biochemistry, Cambridge) for the use of her Flexstation.

REFERENCES

1 Putney, Jr, J. W., Broad, L. M., Braun, F.-J., Lievremont, J.-P. and Bird, G. S. J. (2001) Mechanisms of capacitative calcium entry. J. Cell Sci. **114**, 2223–2229
2 Taylor, C. W. (2002) Controlling calcium entry. Cell **111**, 767–769
3 Shuttleworth, T. J. (2004) Receptor-activated calcium entry channels – who does what, and when? Sci, STKE **pe40**
4 Byron, K. L. and Taylor, C. W. (1993) Spontaneous Ca^{2+} spiking in a vascular smooth muscle cell line is independent of the release of intracellular Ca^{2+} stores. J. Biol. Chem. **268**, 6945–6952
5 Broad, L. M., Cannon, T. R. and Taylor, C. W. (1999) A non-capacitative pathway activated by arachidonic acid is the major Ca^{2+} entry mechanism in rat A7r5 smooth muscle cells stimulated with low concentrations of vasopressin. J. Physiol. **517**, 121–134
6 Moneer, Z. and Taylor, C. W. (2002) Reciprocal regulation of capacitative and non-capacitative Ca^{2+} entry in A7r5 vascular smooth muscle cells: only the latter operates during receptor activation. Biochem. J. **362**, 13–21
7 Putney, Jr, J. W. (2004) Store-operated calcium channels: how do we measure them and do we care? Sci, STKE pe37
8 Thibonnier, M., Bayer, A. L., Simonson, M. S. and Kester, M. (1991) Multiple signaling pathways of V_1-vascular vasopressin receptors of A7r5 cells. Endocrinology **129**, 2845–2856
9 Byron, K. L. and Taylor, C. W. (1995) Vasopressin stimulation of Ca^{2+} mobilization, two bivalent cation entry pathways and Ca^{2+} efflux in A7r5 rat smooth muscle cells. J. Physiol. **485**, 455–468
10 Iwamuro, Y., Miwa, S., Zhang, X.-F., Miowa, T., Enoki, T., Okamoto, Y., Hasegawa, H., Furutani, H., Okazawa, M., Ishikawa, M., Hashimoto, N. and Masaki, T. (1999) Activation of three types of voltage-independent Ca^{2+} channel in A7r5 cells by endothelin-1 as revealed by a novel Ca^{2+} channel blocker LOE-908. Br. J. Pharmacol. **126**, 1107–1114
11 Moneer, Z., Dyer, J. L. and Taylor, C. W. (2003) Nitric oxide co-ordinates the activities of the capacitative and non-capacitative Ca^{2+}-entry pathways regulated by vasopressin. Biochem. J. **370**, 439–448
12 Wicher, D., Messutat, S., Lavaille, C. and Lapied, B. (2004) A new regulation of non-capacitative calcium entry in insect pacemaker neurosecretory neurons: involvement of arachidonic acid, NO-guanylyl cyclase/cGMP, and cAMP. J. Biol. Chem. **279**, 50410–50419
13 Gamberucci, A., Fulceri, R. and Benedetti, A. (1997) Inhibition of store-dependent capacitative Ca^{2+} influx by unsaturated fatty acids. Cell Calcium **21**, 375–385
14 Alonso-Torre, S. R. and García-Sancho, J. (1997) Arachidonic acid inhibits capacitative calcium entry in rat thymocytes and human neutrophils. Biochim. Biophys. Acta **1328**, 207–213
15 Sergeeva, M., Strokin, M., Wang, H., Ubl, J. J. and Reiser, G. (2003) Arachidonic acid in astrocytes blocks Ca^{2+} oscillations by inhibiting store-operated Ca^{2+} entry, and causes delayed Ca^{2+} influx. Cell Calcium **33**, 283–292
16 Luo, D., Broad, L. M., Bird, G. S. J. and Putney, Jr, J. W. (2001) Mutual antagonism of calcium entry by capacitative and arachidonic acid-mediated calcium entry pathways. J. Biol. Chem. **276**, 20186–20189
17 Rychkov, G. Y., Litjens, T., Roberts, M. L. and Barritt, G. J. (2005) Arachidonic acid inhibits store-operated Ca^{2+} current in rat liver cells. Biochem. J. **385**, 551–556
18 Dedkova, E. N. and Blatter, L. A. (2002) Nitric oxide inhibits capacitative Ca^{2+} entry and enhances endoplasmic reticulum Ca^{2+} uptake in bovine vascular endothelial cells. J. Physiol. **539**, 77–91
19 Brueggemann, L. I., Markun, D. R., Barakat, J. A., Chen, H. and Byron, K. L. (2005) Evidence against reciprocal regulation of Ca^{2+} entry by vasopressin in A7r5 aortic smooth muscle cells. Biochem. J. **388**, 237–244
20 Dyer, J. L., Liu, Y., Pino de la Huerga, I. and Taylor, C. W. (2005) Long-lasting inhibition of adenylyl cyclase selectively mediated by inositol 1,4,5-trisphosphate-evoked calcium release. J. Biol. Chem. **280**, 8936–8944

21 Peppiatt, C. M., Holmes, A. M., Seo, J. T., Bootman, M. D., Collins, T. J., McDonald, F. and Roderick, H. L. (2004) Calmidazolium and arachidonate activate a calcium entry pathway that is distinct from store-operated calcium influx in HeLa cells. Biochem. J. **381**, 929–939

22 Lowe, B., Avila, H. A., Bloom, F. R., Gleeson, M. and Kusser, W. (2003) Quantitation of gene expression in neural precursors by reverse-transcription polymerase chain reaction using self-quenched, fluorogenic primers. Anal. Biochem. **315**, 95–105

23 Livak, K. J. and Schmittgen, T. D. (2001) Analysis of relative gene expression data using real-time quantitative PCR and $2^{-\Delta\Delta T}$ method. Methods **25**, 402–408

24 Ostrom, R. S., Liu, X., Head, B. P., Gregorian, C., Seasholtz, T. M. and Insel, P. A. (2002) Localization of adenylyl cyclase isoforms and G protein-coupled receptors in vascular smooth muscle cells: expression in caveolin-rich and noncaveolin domains. Mol. Pharmacol. **62**, 983–992

25 Crossthwaite, A. J., Seebacher, T., Masada, N., Ciruela, A., Dufraux, K., Schultz, J. E. and Cooper, D. M. F. (2005) The cytosolic domains of Ca^{2+}-sensitive adenylyl cyclases dictate their targeting to plasma membrane lipid rafts. J. Biol. Chem. **280**, 6380–6391

26 Broad, L. M., Cannon, T. R., Short, A. D. and Taylor, C. W. (1999) Receptors linked to polyphosphoinositide hydrolysis stimulate Ca^{2+} extrusion by a phospholipase C-independent pathway. Biochem. J. **342**, 199–206

27 Sutherland, C. A. and Amin, D. (1982) Relative activities of rat and dog platelet phospholipase A_2 and diglyceride lipase. J. Biol. Chem. **257**, 14006–14010

28 Doyle, V. M., Creba, J. A., Rüegg, U. T. and Hoyer, D. (1986) Serotonin increases the production of inositol phosphates and mobilises calcium via 5-HT_2 receptor in A7r5 smooth muscle cells. Naunyn-Shmiedeberg's Arch. Pharmacol. **333**, 98–103

29 De Moel, M. P., van de Put, F. H. M. M., Vermegen, T. M. J. A., De Pont, J. J. H. H. M. and Willems, P. H. G. M. (1995) Effect of the aminosteroid, U73122, on Ca^{2+} uptake and release properties of rat liver microsomes. Eur. J. Biochem. **234**, 626–631

30 Ostrom, R. S. (2002) New determinants of receptor–effector coupling: trafficking and compartmentation in membrane microdomains. Mol. Pharmacol. **61**, 473–476

31 Clapham, D. E. (2003) TRP channels as cellular sensors. Nature (London) **426**, 517–524

32 Putney, Jr, J. W. (2004) The enigmatic TRPCs: multifunctional cation channels. Trends Cell Biol. **14**, 282–286

33 Jung, S., Strotmann, R., Schultz, G. and Plant, T. D. (2002) TRPC6 is a candidate channel involved in receptor-stimulated cation currents in A7r5 smooth muscle cells. Am. J. Physiol. Cell Physiol. **282**, C347–C359

34 Inoue, R., Okada, T., Ooue, H., Hara, Y., Shimizu, S., Naitoh, S., Ito, Y. and Mori, Y. (2001) The transient receptor potential homologue TRP6 is the essential component of vascular α_1-adrenoceptor-activated Ca^{2+}-permeable cation channel. Circ. Res. **88**, 325–332

35 Yu, Y., Fantozi, I., Remillard, C. V., Landsberg, J. W., Kunichika, N., Platoshyn, O., Tigno, D. D., Thistlethwaite, P. A., Rubin, L. J. and Yuan, J. X.-J. (2004) Enhanced expression of transient receptor potential channels in idiopathic pulmonary arterial hypertension. Proc. Natl. Acad. Sci. U.S.A. **101**, 13861–13866

36 Plevin, R., Stewart, A., Paul, A. and Wakelam, M. J. O. (1992) Vasopressin-stimulated [^{3}H]-inositol phosphate and [^{3}H]-phosphatidylbutanol accumulation in A10 vascular smooth muscle cells. Br. J. Pharmacol. **107**, 109–115

37 Trebak, M., Hempel, N., Wedel, B. J., Smyth, J. T., Bird, G. S. J. and Putney, Jr, J. W. (2005) Negative regulation of TRPC3 channels by protein kinase C-mediated phosphorylation of serine 712. Mol. Pharmacol. **67**, 558–563

38 Brueggemann, L. I., Martin, B. L., Barakat, J., Byron, K. L. and Cribbs, L. L. (2005) Low-voltage-activated calcium channels in vascular smooth muscle: T-type channels and AVP-stimulated calcium spiking. Am. J. Physiol. Heart Circ. Physiol. **288**, H923–H935

39 Delmas, P., Wanaverbecq, N., Abogadie, F. C., Mistry, M. and Brown, D. A. (2002) Signaling microdomains define the specificity of receptor-mediated $InsP_3$ pathways in neurons. Neuron **34**, 209–220

40 Goligorsky, M. S., Li, H., Brodsky, S. and Chen, J. (2002) Relationship between caveolae and eNOS: everything in proximity and the proximity of everything. Am. J. Physiol. Renal Physiol. **283**, F1–F10

41 Cooper, D. M. F. (2003) Regulation and organization of adenylyl cyclases and cAMP. Biochem. J. **375**, 517–529

42 Clapham, D. E., Runnels, L. W. and Strübing, C. (2001) The TRP ion channel family. Nat. Rev. Neurosci. **2**, 387–396

43 Thyagarajan, B., Poteser, M., Romanin, C., Kahr, H., Zhu, M. X. and Groschner, K. (2001) Expression of Trp3 determines sensitivity of capacitative Ca^{2+} entry to nitric oxide and mitochondrial Ca^{2+} handling: evidence for a role of Trp3 as a subunit of capacitative Ca^{2+} entry channels. J. Biol. Chem. **276**, 48149–48158

44 Zhu, X., Jiang, M. and Birnbaumer, L. (1998) Receptor-activated Ca^{2+} influx via human Trp3 stably expressed in human embryonic kidney (HEK)293 cells: evidence for a non-capacitative Ca^{2+} entry. J. Biol. Chem. **273**, 133–142

45 Mignen, O., Thompson, J. L. and Shuttleworth, T. J. (2001) Reciprocal regulation of capacitative and arachidonate-regulated noncapacitative Ca^{2+} entry pathways. J. Biol. Chem. **276**, 35676–35683

46 Bird, G. S. J. and Putney, Jr, J. W. (2004) Capacitative calcium entry supports calcium oscillations in human embryonic kidney cells. J. Physiol. **562**, 697–706

47 Taylor, C. W. and Tovey, S. (2005) What's in store for Ca^{2+} oscillations? J. Physiol. **562**, 645

Received 21 January 2005/23 May 2005; accepted 26 May 2005
Published as BJ Immediate Publication 26 May 2005, doi:10.1042/BJ20050145